Wettability Pattern for Ultrafast Water Self-Pumping on Cemented Carbide Surface

SUN Pengcheng, HAO Xiuqing, NIU Yusheng, XU Wenhao, LI Liang, HE Ning*

College of Mechanical and Electrical Engineering, Nanjing University of Aeronautics and Astronautics, Nanjing 210016, P. R. China

(Received 9 March 2020; revised 16 April 2020; accepted 20 May 2020)

Abstract: A facile method to fabricate wettability pattern (two extreme wettabilities arranged in a pattern) to realize water self-pumping is proposed on cemented carbide while not necessarily depositing other materials on substrate surface. The water self-pumping is achieved by arranging wedge shaped superhydrophilic domain in superhydrophobic substrate using laser machining. Through single factor experiments, it is found that the key to the extreme wettabilities, micro- and nano-structures, is rendered by laser machining processes and is influenced by laser parameters. Meanwhile, the proper laser parameters that are used to fabricate required micro- and nano-structures are obtained. Finally, the water transport experiment is carried out, which shows that the velocity of water bulge could be up to 362 mm/s when the wedge angle is 3°. The mechanism of the water self-pumping is analyzed and it is found that the migration of water bulge is governed by Laplace pressure of the water bulge induced by the wedge micro-groove.

Key words: wettability pattern; cemented carbide; water self-pumping; micro- and nano-structures; laser machining

CLC number: TN925 **Document code:** A **Article ID:** 1005-1120(2020)03-0416-08

0 Introduction

Surface with wettability pattern has gained wide interests in various fields, such as fog and water collection[1-2], oil/water separation[3], and fundamental biochemical analyses[4], etc. Wettability pattern for liquid transport usually involves wedge shaped surface that, together with its surroundings, are superhydrophilic and can transport liquid[5]. Surface wettability pattern exceeds traditional microfluidics in two aspects: Bypassing complex muti-layer fabrication techniques and avoiding unexpected bubble trapping due to its open nature[6].

Wettability pattern has been widely applied to materials, such as paper[7], glass[8], and metal[9-10], etc., through different techniques, induding photo lithography[11], plasma etching[12], chemical deposition[13], polydimethysiloxane(PDMS)[14], etc. Hong et al.[11] obtained patterned surface for microfluidics through photo lithography by combining the nano morphology and hydrophobicity of polytetrafluoroethylene (PTFE), and the surface can be spin-coated onto glass and polymers. Gau et al.[14] deposited hydrophilic molecules onto a hydrophobic substrate and obtained wettability pattern with high wettability contrast. West et al.[12] and Zimmermann et al.[13] created patterned surface by plasma etching to remove part of hydrophobic domain. Swickrath et al.[15] and Brinkmann et al.[16] printed hydrophilic ink on a hydrophobic substrate to get designed pattern. In summary, all of the aforementioned work need to deposit a functional layer onto the substrate rather than utilize substrate materials themselves. In the latter situation, the wettability pattern layer is easy to be separated from the substrate. Further, these studies strictly rely on substrate surface morphology and surface chemical properties in order to robustly stick the surface with the substrate. Consequently,

*Corresponding author, E-mail address: xqhao@nuaa.edu.cn.

How to cite this article: SUN Pengcheng, HAO Xiuqing, NIU Yusheng, et al. Wettability pattern for ultrafast water self-pumping on cemented carbide surface[J]. Transactions of Nanjing University of Aeronautics and Astronautics, 2020, 37(3): 416-423.

http://dx.doi.org/10.16356/j.1005-1120.2020.03.008

pre-treatment including plasma etching[7] is necessary before deposition.

Water self-pumping on wettability patterned surface could be realized by two means. One is stripe patterning[17-18], where hydrophilic track is stripe; the other is wedge patterning[19]. Although the water transports of the two configurations are both governed by surface tension, they have distinct flow properties. The flow of water in the former is a typical capillary flow (water propagates in a thin film morphology), and governed by capillary force. The flow in the latter is a droplet flow (water propagates in a droplet morphology) and governed by Laplace pressure because water droplet is in a curve during propagation.

We use a facile and portable method to construct a wettability pattern on cemented carbide material that supports water self-pumping. This concept involves the fabrication of micro- and nano-structures on the substrate surface by laser machining technique. And after modification, extreme wettability could be realized through self-assembly. The pattern is designed to be a wedge shape so that water bulge could self-pump under Laplace pressure. The influence of laser parameters on micro- and nano-structures is investigated and the migration of water bulge is also analyzed both theoretically and experimentally. This fabrication method does not need expensive equipment and offers a promising application aspects on metal micro fluidic systems.

1 Materials and Methods

1.1 Materials

The material of samples is a mirror-finished cemented carbide plate (YG8, 5.5 mm thick and 100 mm long, Zhuzhou Cemented Carbide Cutting Tools Co, Ltd). The following chemicals are used for fluorinated treatment: trimethoxysilane, 0.8% (weight fraction) in the corresponding fluorocarbon solvent (Sicong Chemical, China).

1.2 Methods

The pattern is designed to be in wedge shape so that surface tension could serve as a driving force and in this way, water self-pumping could be realized. The fabrication of wettability pattern in this paper can be divided into several steps, as shown in Fig.1. In step 1, the laser beam scanning in the open air (20 min) imparts the required micro- and nano-structures on whole cemented carbide surface, making it possible to decrease the surface energy. Note that laser scanning renders original hydrophilic surface to superhydrophilic due to the formation of micro- and nanostructures, as shown in Fig.1(a). In step 2, the micro- and nano-structured sample is immersed in the fluoride solution for 30 min to decrease surface energy and heated in the vacuum oven with 280 °C to decrease the surface free energy, as shown in Figs.1(b) and (c). The aforementioned steps make the cemented carbide from superhydrophilic to superhydrophobic. In step 3, a designed wedge shaped track is fabricated on the superhydrophobic substrate by laser scanning (10 min), as shown in Fig.1(d). In this step, the laser scanning is used to remove the part of the superhydrophobic surface and the newly exposed wedge groove is superhydrophilic. In this way, a wettability pattern is fabricated on the cemented carbide surface and the total time is 60 min. The main purpose of steps 1 and 2 is to fabricate a superhydrophobic layer. Thus these two steps could be integrated into one step, which is called the under-liquid laser machining[20-21]. For severe friction application area, the under-liquid laser machining method could improve not only the robustness of wettability pattern, but also the manufacturing efficiency.

To investigate the influence of laser parameters on micro- and nano-structures, a single factor method is adapted. While studying the influence of the single pulse energy, the scanning speed v is set to 4 mm/s, times of scanning is set to 5, and the single pulse energy (τ) range is 0.25 mJ to 0.45 mJ. Meanwhile, while studying the influence of scanning speed, the scanning times is set to 5, the single pulse energy is set to 0.35 mJ, and the scanning speed range is 2 mm/s to 64 mm/s.

Scanning electronic microscopy (SEM, S-3400N, Hitachi, Japan) is performed for visual

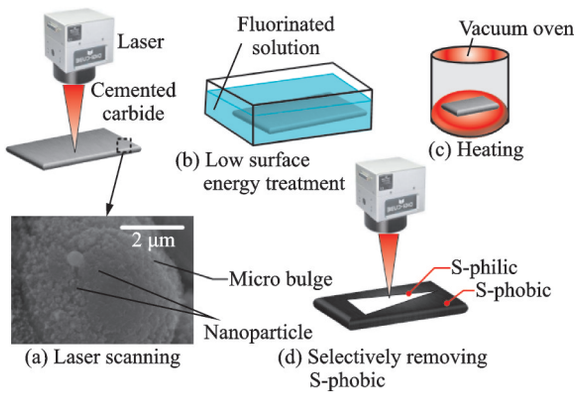

Fig.1 Fabrication process and SEM of required micro- and nano-structures

characterization of the micro- and nano-structures. Wettability characterization is accomplished by a contact angle meter (OCA25HTV, Dataphysics, German). A 6 μL drop of water is dispensed onto the surface and 10 spots are selected to measure the water contact angle (WCA). And the final value is obtained by averaging the aforementioned data.

During the experiment, a 30 μL drop of water is dispensed perpendicularly onto the narrow end of wedge without any initial speed. A high-speed camera is set on the top of the sample to record the migration of water droplet. Meanwhile, another high-speed camera is also set on the side view to capture the droplet migration. And the migration speed is obtained by measuring the displacement in a given amount frames in the record of the top view camera.

2 Results and Discussion

2.1 Influence of single pulse energy on micro- and nano-structures

Fig.2 depicts the variation of surface morphologies as τ increases. Overall, as the pulse energy reaches the surface of cemented carbide, the material of the surface is heated rapidly and some of them are melted and when single pulse ends, the melted materials cool down and turn into solid phase, as shown in Figs.2(a) and (b). As τ keeps increasing, the temperature even exceeds the boiling point and the materials are in an overheated condition. According to Rabelon equation[22], the pressure of vapor on the surface is higher than that in the atmosphere. Under this condition, the vapor pressure serves as a driving force that makes the metallic vaporization escape from material substrate and thrust the metallic vaporization at the same time. As the thrust force exceeds the viscous force (the surface tension of materials), the materials will finally be eliminated from the molten pool, as shown in Figs.2(c)—(e). Further, as τ increases, the material temperature also increases to the thermodynamic critical temperature, and phase explosion occurs where the density of bubble increases until it reaches a critical value[22]. Thus the materials on the surface are transferred into the mixture of vapor and tiny droplets and finally escape from the surface through phase explosion. When a single pulse ends, the temperature on the surface will decrease significantly and turn into micro- and nano-structures, as shown in Fig.2(f). In summary, a high single pulse energy could result in more required micro- and nano-structures. In this paper, 0.45 mJ single pulse energy is adapted to fabricate required micro- and nano-structures.

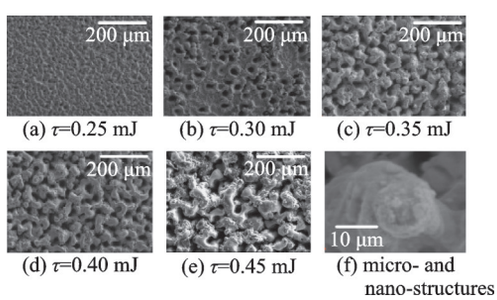

Fig.2 Influence of single pulse energy on surface morphology

2.2 Influence of scanning speed on micro- and nano-structures

Fig.3 shows the surface morphology as scanning speed v increases. A low scanning speed is easier for the formation of micro- and nano-structures. However, as v increases, less micro- and nano-structures are observed. The number of pulse in a unit laser spot N can be calculated by

$$N = \frac{f \times d}{v}$$

where f, d and v are the laser frequency, laser spot diameter, and laser scanning speed, respectively. N is inversely proportional to v, indicating higher energy in a given spot when v decreases. Thus, phase explosion tends to occur under a low scanning speed and the micro- and nano-structures form. When scanning speed increases, less molten pools are observed, as shown in Fig.3(c). However, when scanning speed increases to 64 mm/s, the part of the surface stays intact without any sign of etching, as shown in Fig.3(e). It may be caused by non-uniformity of heat transfer. The part of the material reaches a higher temperature and thus leads to molten phenomenon while other materials of the surface stay in a low temperature and consequently stay intact. In summary, a low scanning speed could result in more required micro- and nano-structures. Consequently, the scanning speed is set to 2 mm/s in this paper. As a result, the laser parameters to fabricate both domains can be found in Table 1.

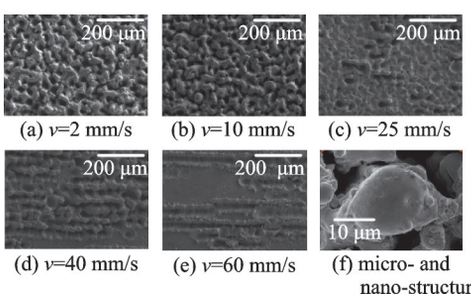

Fig.3 Influence of scanning speed (v) on the surface morphology

Table 1 Laser parameters for fabricating the wettability pattern

Laser parameter	τ/mJ	v/(mm•s^{-1})	Laser scanning times
Value	0.45	2	1

2.3 Water bulge migration

During the last fabrication step, the superhydrophobic layer is removed so that the superhydrophilic area is approximately in a depth of 5 μm. Consequently, distinct from the conventional wettability pattern, the superhydrophilic area in this paper is not on the same plane with the superhydrophobic area. Thus the pinning effect and wettability contrast ensure that the water can be transported along the wedge groove.

A wedge groove with a wedge angle of 3° is initially chosen. Time-lapse images from side view in Fig.4 show different stages for a water droplet migration. After contacting with the narrow end of the wedge, the water quickly changes into the shape of an asymmetric semi-ellipse where the leading front is in a shape of meniscus, as shown in Fig.4(b). The top view shows that the leading area of the droplet is totally confined inside the wedge groove and advanced in front of the bulge with a higher velocity, which may be attributed to hemiwicing[23], a phenomenon influenced by the micro-pillars in the superhydrophilic domain. As the propagation continues, the height of bulge decreases constantly and a long trailing area is also observed. Finally, the bulge takes the shape of semi-cone. The velocity of leading front slows down until the leading front reaches the wide end, as shown in Fig.4(e). Ref.[24] investigated that the critical condition for the bulge morphology shift is determined by the width of track and the volume of the bulge. In this paper, more attention is focused on the bulge advancement rather than the whole process. Thus the bulge migration can be found in Fig.5(red area). And the blue area denotes the semi-cone migration. The red line denotes the fitted velocity curve. As shown in the red area, advancement of the bulge is accelerated until it reaches the maximum velocity (350 mm/s). This indicates an ultrafast high transport velocity compared with the water transport velocity on the wettability pattern fabricated using deposition[25] or coating techniques[26]. And then it begins to slow down due to the morphology shift. However, with the increase of time, the acceleration decreases, indicating that the net driving force decreases with the propagation of water bulge.

In the process of spreading, the bulge continuously touches the wettability boundary (the bound-

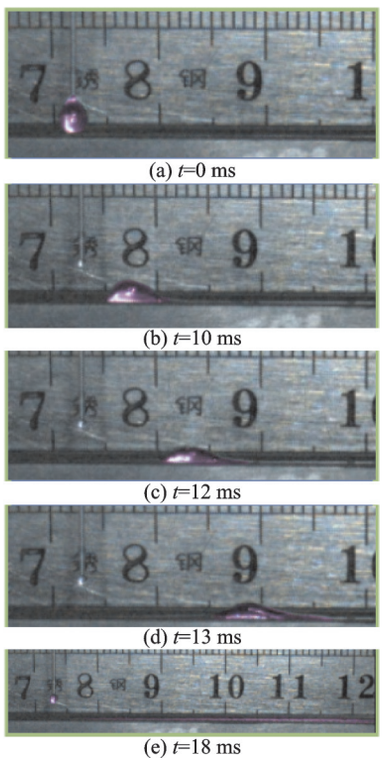

Fig.4 Real time-lapsed images (side view) of water bulge propagation

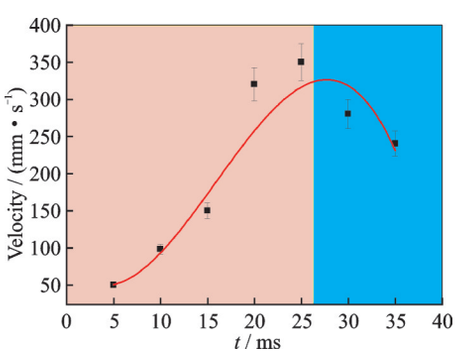

Fig.5 Variation of velocity (Red area denotes the migration of water bulge while blue area denotes thin water film after bulge morphology shifting)

ary between superhydrophilic and superhydrophilic domain is also known as triple-line), thus the Laplace pressure is served as a source of the driving force that propels the droplet to the wide end. Because the migration is on the thin water film, the viscous force is ignored in this paper. At the same time, the Laplace pressure difference between the leading and trailing area also induces a driving force, as shown in Fig.6. Laplace pressure changes with the advancement of bulge, thus the velocity is closely affected by Laplace pressure. As a result, Laplace pressure and velocity will change in a same behavior.

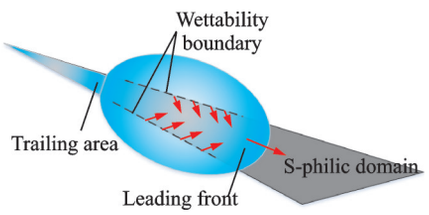

Fig.6 Schematic illustration of driving force for the propagation of water bulge

Theoretically, spreading of water droplets is inevitable as it always seeks to minimize the free energy of the whole system and the net driving force may be obtained by taking the axial deviation of free energy[5]

$$F_d = -\frac{\mathrm{d}}{\mathrm{d}x}(\sigma_{\mathrm{LG}} A_{\mathrm{LG}} + \sigma_{\mathrm{LS}} A_{\mathrm{LS}} + \sigma_{\mathrm{SG}} A_{\mathrm{SG}})$$

where σ_{ij} denotes the surface tension per unit interface area between liquid (L), gas (G) and solid (S), and A_{ij} the corresponding area value. Apparently, A_{ij} is difficult to measure. To simplify model, another mathematical model must be developed. The propagation of droplets is governed by Laplace pressure induced from liquid/solid interface along with the wedge side[5]. The propogation would be impossible if the droplet is in a stripe superhydrophilic track[24]. Thus the net driving force could be obtained by taking the deviation of Laplace pressure lengthwise[5,18].

The local Laplace pressure can be obtained by

$$\Delta p \sim \frac{2\sigma}{r}$$

where σ denotes the surface tension and r the bulge radius. The radius of bulge at a local area $r(x)$ can be obtained by

$$r(x) = \frac{\delta(x)}{2\sin\theta(x)}$$

where $\delta(x)$ is the local width of the wedge. Apparently, Young's equation is no longer suitable due to continuous touch with the wettability boundary of bulge[21]. However, WCA $\theta(x)$ can be considered as higher than that in the superhydrophilic domain ($\theta_{\text{S-philic}} \approx 2°$) and lower than that in the superhydro-

phobic domain ($\theta_{S\text{-phobic}} \approx 152°$). Here, considering a fitting value and the local Laplace pressure can be expressed by

$$\Delta p \sim \frac{4\sigma \sin\theta_{fit}}{x \tan\alpha}$$

where x is the displacement and α the wedge angle. Thus, the driving force could be obtained by[5,18]

$$F_d \sim -\frac{d\Delta p}{dx} \sim \frac{4\sigma \sin\theta_{fit}}{x^2 \tan\alpha}$$

The calculation indicates that, during the advancement of bulge, the driving force will decrease and the acceleration will decrease, which is consistent with the observation in Fig.5. The acceleration (the slop value of the fitting function) in Fig.5 decreases, indicating a decrease of Laplace pressure gradient.

3 Conclusions

A new method to fabricate wettability pattern (wedge shaped superhydrophilic track with superhydrophobic domain surrounded) on cemented carbide has been demonstrated using laser machining technique. The micro- and nano-structure, which was formed during laser irradiation and was responsible for the extreme wettability properties, has been analyzed under different laser parameters. It was found that the micro- and nano-structure tended to be formed under low scanning speed as well as intense laser pulse energy.

During water transport experiments, the water droplet could be transported pumplessly with an ultrafast speed and it was found that the advancement of water bulge was accelerated by the Laplace pressure along the triple-line and at the same time, under the Laplace difference between the leading and trailing area of water bulge, which was also in consistent with the observation in Fig.5. The Laplace gradient decreased with the propagation of water bulge, resulting in a decrease of transport acceleration. In summary, the new fabrication method offers a promising prospect for wettability pattern construction on metal surface, especially metals, such as iron, aluminum as well as alloys.

References

[1] LU Y. Superhydrophilic-superhydrophobic patterned surfaces on glass substrate for water harvesting[J]. Journal of Materials Science, 2020, 55(2): 1-11.

[2] PARKER A R, LAWRENCE C R. Water capture by a desert beetle[J]. Nature, 2001, 414(6859): 33-34.

[3] CHU Z, FENG Y, SEEGER S. Oil/water separation with selective superantiwetting/superwetting surface materials[J]. Angewandte Chemie International Edition, 2015, 54(8): 2328-2338.

[4] SCHUTZIUS T M, ELSHARKAWY M, TIWARI M K, et al. Surface tension confined (STC) tracks for capillary-driven transport of low surface tension liquids[J]. Lab on a Chip, 2012, 12(24): 5237-5242.

[5] GHOSH A, GANGULY R, SCHUTZIUS T M, et al. Wettability patterning for high-rate, pumpless fluid transport on open, non-planar microfluidic platforms[J]. Lab on a Chip, 2014, 14(9): 1538-1550.

[6] HONG L, PAN T. Three-dimensional surface microfluidics enabled by spatiotemporal control of elastic fluidic interface[J]. Lab on a Chip, 2010, 10(23): 3271-3276.

[7] BALU B, BERRY A D, HESS D W, et al. Patterning of superhydrophobic paper to control the mobility of micro-liter drops for two-dimensional lab-on-paper applications[J]. Lab on a Chip, 2009, 9(21): 3066-3075.

[8] FENG W, BHUSHAN B. Multistep wettability gradient in bioinspired triangular patterns for water condensation and transport[J]. Journal of Colloid and Interface Science, 2020, 560: 866-873.

[9] HIRAI Y, MAYAMA H, MATSUO Y, et al. Uphill water transport on a wettability-patterned surface: Experimental and theoretical results[J]. ACS Applied Materials & Interfaces, 2017, 9(18): 15814-15821.

[10] CHOI W T, YANG X, BREEDVELD V, et al. Creation of wettability contrast patterns on metallic surfaces via pen drawn masks[J]. Applied Surface Science, 2017, 426: 1241-1248.

[11] HONG L, PAN T. Photopatternable superhydrophobic nanocomposites for microfabrication[J]. Journal of Microelectromechanical Systems, 2010, 19(2): 246-253.

[12] WEST J, MICHELS A, KITTEL S, et al. Microplasma writing for surface-directed millifluidics[J].

Lab on a Chip, 2007, 7(8): 981-983.

[13] ZIMMERMANN M, HUNZIKER P, DELAMARCHE E. Valves for autonomous capillary systems[J]. Microfluidics and Nanofluidics, 2008, 5(3): 395-402.

[14] GAU H, HERMINGHAUS S, LENZ P, et al. Liquid morphologies on structured surfaces: From microchannels to microchips[J]. Science, 1999, 283(5398): 46-49.

[15] SWICKRATH M J, BURNS S D, WNEK G E. Modulating passive micromixing in 2-D microfluidic devices via discontinuities in surface energy[J]. Sensors and Actuators B: Chemical, 2009, 140(2): 656-662.

[16] BRINKMANN M, LIPOWSKY R. Wetting morphologies on substrates with striped surface domains[J]. Journal of Applied Physics, 2002, 92(8): 4296-4306.

[17] XING S, HARAKE R S, PAN T. Droplet-driven transports on superhydrophobic-patterned surface microfluidics[J]. Lab on a Chip, 2011, 11(21): 3642-3648.

[18] SEN U, CHATTERJEE S, GANGULY R, et al. Scaling laws in directional spreading of droplets on wettability-confined diverging tracks[J]. Langmuir, 2018, 34(5): 1899-1907.

[19] READY J F. Effects due to absorption of laser radiation[J]. Journal of Applied Physics, 1965, 36(2): 462-468.

[20] XIAO Sinong, HAO Xiuqing, YANG Yinfei, et al. Feasible fabrication of a wear-resistant hydrophobic surface[J]. Applied Surface Science, 2018. DOI: 10.1016/j.apsusc.2018.09.030.

[21] HAO Xiuqing, SUN Pengcheng, XIAO Sinong, et al. Tribological performance of surface with different wettability under ball-ondisc test[J]. Applied Surface Science, 2020, 501: 144228.

[22] CHEN H, ZANG H, LI X, et al. Toward a better understanding of hemiwicking: A simple model to comprehensive prediction[J]. Langmuir, 2019, 35(7): 2854-2864.

[23] LENZ P, LIPOWSKY R. Morphological transitions of wetting layers on structured surfaces[J]. Physical Review Letters, 1998, 80(9): 1920-1923.

[24] BRINKMANN M, LIPOWSKY R. Wetting morphologies on substrates with striped surface domains[J]. Journal of Applied Physics, 2002, 92(8): 4296-4306.

[25] NAKASHIMA Y, NAKANISHI Y, YASUDA T. Automatic droplet transportation on a plastic microfluidic device having wettability gradient surface[J]. Review of Scientific Instruments, 2015, 86(1): 015001.

[26] WU H, ZHU K, CAO B, et al. Smart design of wettability-patterned gradients on substrate-independent coated surfaces to control unidirectional spreading of droplets[J]. Soft Matter, 2017, 13(16): 2995-3002.

Acknowledgements This work was supported by the National Natural Science Foundation of China (No.51875285), the Natural Science Foundation of Jiangsu Province (No.BK20190066), the Fundamental Research Funds for the Central Universities (No.NE2020005), and the Foundation of the Graduate Innovation Center, Nanjing University of Aeronautics and Astronautics (No. kfjj20190508).

Authors Mr. **SUN Pengcheng** received his B.S. degree of Mechanical Engineering from Shandong University, Jinan, China, in 2014. In September 2018, he joined the advanced cutting technology (ACT) Lab in College of Mechanical and Electrical Engineering (CMEE), Nanjing University of Aeronautics and Astronautics (NUAA). His research interests focus on microfluidics, surface tribology, and micro/nano manufacturing technology.

Dr. **HAO Xiuqing** received her B.S. degree from Chongqing University, Chongqing, China, in 2007. She received her Ph.D. degree of Mechanical Engineering from Xi'an Jiaotong University, Xi'an, China, in 2014. From 2012 to 2013, she was a visiting scholar in the department of Mechanical Engineering, Northwestern University, Evanston, USA. She is an associate professor of CMEE, NUAA. Her research interests focus on micro/nano manufacturing technology, friction reduction, surface tribology and surface wetting behavior.

Author contributions Mr. **SUN Pengcheng** conducted the analysis, interpreted the results, and revised the manuscript. Dr. **HAO Xiuqing** designed the study and the experimental setup, and revised the manuscript. Mr. **SUN Pengcheng** and Mr. **NIU Yusheng** conducted the experiments, and wrote the manuscript. Mr. **XU Wenhao** analyzed the surface morphology. Profs. **LI Liang** and **HE Ning** contributed to the discussion and background of the study. All authors have discussed on the manuscript draft and approved the submission.

Competing interests The authors declare no competing interests.

(Production Editor: XU Chengting)

硬质合金润湿图案化表面的超快无泵水自输运特性研究

孙鹏程，郝秀清，牛宇生，徐文豪，李 亮，何 宁

(南京航空航天大学机电学院,南京 210016,中国)

摘要:提出了一种在硬质合金表面制备可以实现水自输送的润湿图案化表面的方法,即激光加工法,该方法可以不需要在基底表面上沉积材料。该润湿图案化表面包含楔形超亲液沟槽以及外围的超疏液表面,借助该图案化表面,液滴可以实现快速自输送。通过单因素试验发现,导致硬质合金表面极端润湿的关键因素是激光加工过程中产生的微纳织构,且微纳织构的形成受激光加工参数的影响。与此同时,通过单因素试验找到了微纳织构产生的合理激光加工参数。最后,通过水滴运输实验发现,当超亲液的楔形槽楔角是3°时,该润湿图案化表面对水的运输速度能够达到362 mm/s。还分析了水在该表面上的运输机制,发现水的自驱动运输是由图案化表面引起的水滴自身拉普拉斯压力梯度控制的。

关键词:润湿图案;硬质合金;水自输送;微纳织构;激光加工